

Articles

Stereoselective Synthesis of *ortho*-Carbaborane-Containing *P*-Chiral Phosphanlyferrocenes[†]

Steffen Tschirschwitz, Peter Lönnecke, and Evamarie Hey-Hawkins*

Institut für Anorganische Chemie der Universität Leipzig, Johannisallee 29, D-04103 Leipzig, Germany

Received May 22, 2007

Diastereomerically pure 1-[1-(1,2-dicarba-*closo*-dodecaboran(12)yl)chlorophosphanlyl]-2-*N,N*-dimethylaminomethylferrocene ((*R*_P,*S*_{FC}/*S*_P,*R*_{FC})-**3**) and enantiomerically pure (*S*)-*N,N*-dimethyl-1-[(*R*)-2-[(*S*)-1-(1,2-dicarba-*closo*-dodecaboran(12)yl)]chlorophosphanlyl]ferrocenyl]ethylamine ((*S*_C,*S*_P,*R*_{FC})-**4**) were prepared by reaction of monolithiated 1,2-dicarba-*closo*-dodecaborane(12) and the corresponding racemic or enantiomerically pure aminoalkylferrocenyldichlorophosphanes (**1** or (*S,R*)-**2**). Two equivalents of **1** also reacted with dilithiated 1,2-dicarba-*closo*-dodecaborane(12) to yield stereoselectively the *R*_P,*R*_P,*S*_{FC},*S*_{FC}/*S*_P,*S*_P,*R*_{FC},*R*_{FC} diastereomer of 1,2-bis[chloro(2-*N,N*-dimethylaminomethylferrocenyl)phosphanlyl]-1,2-dicarba-*closo*-dodecaborane(12) ((*R*_P,*R*_P,*S*_{FC},*S*_{FC}/*S*_P,*S*_P,*R*_{FC},*R*_{FC})-**5**). Chlorophosphane (*R*_P,*S*_{FC}/*S*_P,*R*_{FC})-**3** was treated with LiAlH₄ to afford diastereoselectively the secondary phosphane 1-[1-(1,2-dicarba-*closo*-dodecaboran(12)yl)phosphanlyl]-2-*N,N*-dimethylaminomethylferrocene ((*R*_P,*R*_{FC}/*S*_P,*S*_{FC})-**6**) with inverted stereochemistry at the phosphorus center, which in this case was found to slowly undergo epimerization in solution. The chloro groups of (*R*_P,*S*_{FC}/*S*_P,*R*_{FC})-**3** and (*S*_C,*S*_P,*R*_{FC})-**4** were also substituted by various alkoxides to give a series of diastereomerically and enantiomerically pure carbaboranylferrocenyl phosphinites ((*R*_P,*R*_{FC}/*S*_P,*S*_{FC})-**7**, (*R*_P,*R*_{FC}/*S*_P,*S*_{FC})-**8**, (*R*_P,*R*_{FC}/*S*_P,*S*_{FC})-**9**, (*S*_C,*R*_P,*R*_{FC})-**10**, and (*S*_C,*R*_P,*R*_{FC})-**11**). The substitutions occurred with 100% stereoselective inversion of the configurations of the phosphorus centers. The phosphinites display high stability toward oxidation and epimerization. All new compounds were structurally characterized to verify the configurations of the stereogenic centers. The monophosphanlyl-substituted carbaboranes exhibit intramolecular hydrogen-bonding interactions between the dimethylamino group and the proton of the second cluster carbon atom.

Introduction

Ferrocene has proved to be a versatile substituent for phosphanes because of its rich chemistry, stability, and redox properties.¹ As a consequence, phosphorus-substituted aminoalkylferrocenes have attracted great interest since Hayashi et al. prepared (*R,S*)-PPFA ((*R*)-*N,N*-dimethyl-1-[(*S*)-2-(diphenylphosphino)ferrocenyl]ethylamine), the first optically pure derivative of this class of compounds that combine central and planar chirality.² Its synthesis was made possible after Ugi et al. had developed a method to prepare enantiopure *N,N*-dimethyl-1-ferrocenylethylamine, now known as Ugi's amine,³ which has become one of the most important chiral starting materials in ferrocene chemistry, as its central chirality induces diastereoselective *ortho* lithiation leading to defined planar chirality. The class of chiral aminoalkylferrocenylphosphanes has been growing ever since, because many of these compounds

were found to be excellent ligands for transition metals in homogeneous catalysis.^{2,4} Besides their ability to induce stereoselectivity, planar-chiral aminoalkylferrocenylphosphanes have other characteristics that make them versatile. They can be further modified in different ways, for example, by substitution of the amino group or functionalization of the second Cp ring.⁵ Their planar chirality is extremely stable toward racemization, and most of the known catalytically active compounds, for instance, Josiphos,⁶ Walphos,⁷ and Mandypfos,⁸ are stable, quite readily accessible, and easy to handle. In contrast to the

[†] Parts of these results were previously reported at the XXII ICOMC in Zaragoza, Spain, July 23–28, 2006, as a poster (P47) presentation.

* Corresponding author. E-mail: hey@rz.uni-leipzig.de.

(1) For an overview, see: *Ferrocenes. Homogeneous Catalysis, Organic Synthesis, Materials Science*; Togni, A., Hayashi, T., Eds.; VCH: Weinheim 1995.

(2) Hayashi, T.; Yamamoto, K.; Kumada, M. *Tetrahedron Lett.* **1974**, 4405.

(3) Marquading, D.; Klusacek, H.; Gokel, G. W.; Hoffmann, P.; Ugi, I. *K. J. Am. Chem. Soc.* **1970**, 92, 5389.

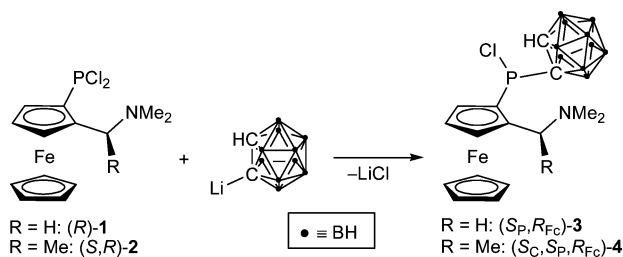
(4) (a) Hayashi, T.; Mise, T.; Fukushima, M.; Kagotani, M.; Nagashima, N.; Hamada, Y.; Matsumoto, A.; Kawakami, S.; Konishi, M.; Yamamoto, K.; Kumada, M. *Bull. Chem. Soc. Jpn.* **1980**, 53, 1138. (b) Cullen, W. R.; Woollins, J. D. *Can. J. Chem.* **1982**, 60, 1793. (c) Hayashi, T.; Tajika, M.; Tamao, K.; Kumada, M. *J. Am. Chem. Soc.* **1976**, 98, 3718. (d) Colacot, T. *J. Chem. Rev.* **2003**, 103, 3101.

(5) (a) Richards, C. J.; Locke, A. J. *Tetrahedron: Asymmetry* **1998**, 9, 2377. (b) Togni, A.; Bieler, N.; Burckhardt, U.; Köllner, C.; Pioda, G.; Schneider, R.; Schnyder, A. *Pure Appl. Chem.* **1999**, 71, 1531. (c) Sutcliffe, O. B.; Bryce, M. R. *Tetrahedron: Asymmetry* **2003**, 14, 2297. (d) Barbaro, P.; Bianchini, C.; Giambastiani, G.; Parisel, S. L. *Coord. Chem. Rev.* **2004**, 248, 2131. (e) Gómez Arrayás, R.; Adrio, J.; Carretero, J. C. *Angew. Chem.* **2006**, 118, 7836; *Angew. Chem., Int. Ed.* **2006**, 45, 7674.

(6) Togni, A.; Breutel, C.; Schnyder, A.; Spindler, F.; Landert, H.; Tijani, A. *J. Am. Chem. Soc.* **1994**, 116, 4062.

(7) Weissensteiner, W.; Sturm, T.; Spindler, F. *Adv. Synth. Catal.* **2003**, 345, 160.

(8) Perea, A. J. J.; Borner, A.; Knochel, P. *Tetrahedron Lett.* **1998**, 39, 8073.

Scheme 1. Only the Formation of (S_P, R_{FC})-**3** Is Shown

large number of ferrocenylphosphanes combining planar and carbon-centered chirality, much less attention has been paid to additional phosphorus-centered chirality.⁹ As demonstrated by the great success of Dipamp,¹⁰ a chiral center directly at the donor atom of a metal complex, that is, in the closest possible proximity to the catalytic center, is very likely to enhance the stereoselectivity of an asymmetric homogeneous catalysis reaction.

Another interesting substituent in phosphanes, beside a ferrocenyl group, is the 1,2-dicarba-*closo*-dodecaborane(12) (*ortho*-carbaborane) moiety. The hydrogen atoms at the cage carbon atoms are acidic and can be removed by strong bases to facilitate a wide variety of substitution reactions.¹¹ Furthermore, the highly electron-withdrawing *ortho*-carbaborane cluster changes the electronic properties of the substituents drastically, and the steric influence is also of interest.¹² Carbaboranyl phosphanes have been known since 1963 and are easily accessible by reaction of the mono- or dilithiated carbaborane with chlorophosphanes.¹³ A number of derivatives have been prepared in this way, and several have successfully been applied as ligands in homogeneous catalysis.¹⁴ However, most research focuses on disubstituted derivatives in which the carbaboranyl group acts as a rigid backbone for chelating ligands.^{11a,12,15}

Recently, we presented a method to prepare a series of racemic and enantiomerically pure aminoalkylferrocenyldichlorophosphanes.¹⁶ We herein show that one chloro group of these compounds can easily be substituted by reaction with monolithiated 1,2-dicarba-*closo*-dodecaborane(12) as nucleophile with very high diastereoselectivity. The remaining chloro group of

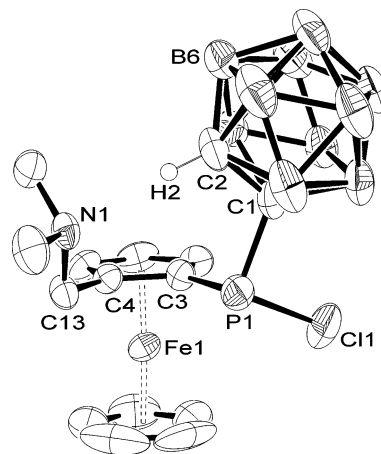


Figure 1. Molecular structure and atom-labeling scheme for the S_P, R_{FC} enantiomer of ($R_P, S_{FC}/S_P, R_{FC}$)-**3**, with thermal ellipsoids at the 50% probability level. Only one of two crystallographically independent molecules present in the asymmetric unit is shown. H atoms except H2 are omitted for clarity.

these *P*-chiral ferrocenylcarbaboranylchlorophosphanes can also be substituted with complete inversion of the chirality at phosphorus. Nonchiral and chiral alkoxides as well as a hydride were chosen as substituents. All presented new compounds have been characterized by X-ray analysis.

Results and Discussion

To prepare the desired carbaboranylferrocenylchlorophosphanes, monolithiated 1,2-dicarba-*closo*-dodecaborane(12) was treated with racemic or enantiopure aminoalkylferrocenyldichlorophosphanes (Scheme 1). In the case of racemic 1-dichlorophosphanyl-2-*N,N*-dimethylaminomethylferrocene (**1**), the obtained product **3** is a single diastereomer that consists of the two enantiomers (R_P, S_{FC})-**3** and (S_P, R_{FC})-**3**, as verified by X-ray diffraction analysis. The second diastereomer could be detected only in trace amounts by $^{31}\text{P}\{^1\text{H}\}$ NMR spectroscopy. It could not be isolated and was easily removed by recrystallization. It therefore can be shown that the planar chirality dictates the chirality at the *P* center. In this case *R* configuration at the substituted cyclopentadienyl ring induces *S* configuration at the phosphorus center, and an *S*-configured ring leads to *R*-configured *P* chirality. Hence, the use of enantiomerically pure (*S*)-*N,N*-dimethyl-1-[(*R*)-2-(dichlorophosphanyl)ferrocenyl]-ethylamine ((*S,R*)-**2**) as starting material gives enantiomerically pure (S_C, S_P, R_{FC})-**4** with well-defined chirality at the *P* atom, that is, with the same chiral-induction effect as observed for ($R_P, S_{FC}/S_P, R_{FC}$)-**3**. The second enantiomer, (R_C, R_P, S_{FC})-**4**, can be obtained analogously by using (*R,S*)-**2** as starting material.

Ferrocenylcarbaboranylchlorophosphanes **3** and **4**, which to the best of our knowledge are the first carbaboranyl-substituted ferrocenylphosphanes, were characterized by X-ray diffraction. In this way the influence of the planar chirality on the *P* chirality could be studied, and the absolute configuration of each stereocenter determined. The molecular structure of (S_P, R_{FC})-**3** is depicted in Figure 1; selected bond lengths and angles are given in Table 1. The geometrical environment of the phosphorus atom is distorted tetrahedral. In comparison to known carbaboranylchlorophosphanes, the *P*–Cl and *P*–C bond lengths are within the same range, while the *P*–C3 bond is slightly shorter.^{11b,c} The bond angles C1–P1–C3, C1–P1–Cl1, C3–P1–Cl1, and C2–C1–P1 are also not significantly different. The dimethylamino group is bent toward the carbaborane cluster, which is situated above the substituted cyclopentadienyl ring,

(9) (a) For a recent overview see: Grabulosa, A.; Granell, J.; Müller, G. *Coord. Chem. Rev.* **2007**, *251*, 25. (b) Butler, I. R.; Cullen, W. R.; Rettig, S. J. *Organometallics* **1986**, *5*, 1320. (c) Togni, A.; Breutel, C.; Soares, M. C.; Zanetti, N.; Gerfin, T.; Gramlich, V.; Spindler, F.; Rihs, G. *Inorg. Chim. Acta* **1994**, *222*, 213. (d) Troitskaya, L. L.; Starikova, Z. A.; Demeshchik, D. V.; Sokolov, V. I. *Russ. Chem. Bull.* **1999**, *48*, 1738. (e) Nettekoven, U.; Widhalm, M.; Kamer, P. C. J.; van Leeuwen, P. W. N. M.; Mereiter, K.; Lutz, M.; Spek, A. L. *Organometallics* **2000**, *19*, 2299. (f) Barbaro, P.; Bianchini, C.; Giambastiani, G.; Togni, A. *Chem. Commun.* **2002**, 2672. (g) Chen, W.; Mbafor, W.; Roberts, S. M.; Whittall, J. J. *Am. Chem. Soc.* **2006**, *128*, 3922.

(10) Knowles, W. S.; Sabacky, M. J.; Vineyard, B. D.; Weinkauff, D. J. *J. Am. Chem. Soc.* **1975**, *97*, 2567.

(11) (a) Bregadze, V. I. *Chem. Rev.* **1992**, *92*, 209. (b) Balema, V. P.; Blaurock, S.; Hey-Hawkins, E. *Polyhedron* **1999**, *18*, 545. (c) Sterzig, A.; Rys, E. G.; Blaurock, S.; Hey-Hawkins, E. *Polyhedron* **2001**, *20*, 3007.

(12) Paavola, S.; Teixidor, F.; Viñas, C.; Kivekäs, R. *J. Organomet. Chem.* **2002**, *645*, 39, and references therein.

(13) (a) Alexander, R. P.; Schroeder, H. *Inorg. Chem.* **1963**, *2*, 1107. (b) Godovikov, N. N.; Balema, V. P.; Rys, E. G. *Russ. Chem. Rev.* **1997**, *66*, 1017.

(14) (a) Hart, F. A.; Owen, D. W. *Inorg. Chim. Acta* **1985**, *103*, L1. (b) Longato, B.; Bresadola, S. *Inorg. Chem.* **1982**, *21*, 168. (c) Lee, H.-S.; Bae, J.-Y.; Kim, D.-H.; Kim, H. S.; Kim, S.-J.; Cho, S.; Ko, J.; Kang, S. O. *Organometallics* **2002**, *21*, 210. (d) Wang, H.; Chan, H.-S.; Okuda, J.; Xie, Z. *Organometallics* **2005**, *25*, 3118.

(15) (a) *Metal Complexes in Cancer Chemotherapy*; Keppler, B. K., Ed.; VCH: Weinheim, New York, 1993. (b) Balema, V. P.; Somoza, F., Jr.; Hey-Hawkins, E. *Eur. J. Inorg. Chem.* **1998**, 651.

(16) Tschirschwitz, S.; Lönnecke, P.; Hey-Hawkins, E. *Dalton Trans.* **2007**, 1377.

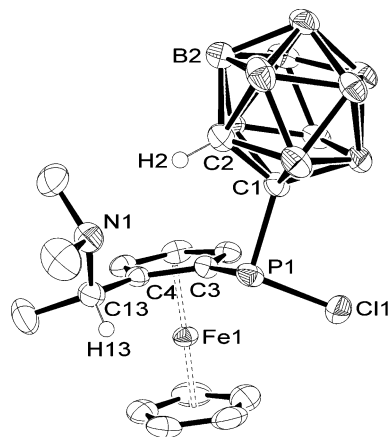
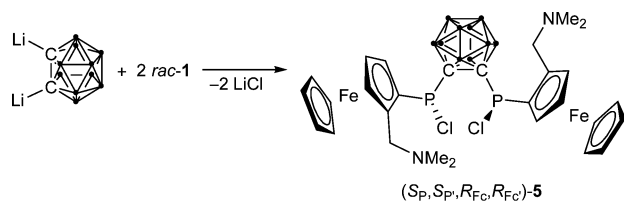


Figure 2. Molecular structure and atom-labeling scheme for (S_C, S_P, R_{Fc})-**4** with thermal ellipsoids at the 50% probability level. H atoms except H2 and H13 are omitted for clarity.

Table 1. Selected Bond Lengths (Å) and Angles (deg) for ($R_P, S_{Fc}/S_P, R_{Fc}$)-**3** and (S_C, S_P, R_{Fc})-**4**

	($R_P, S_{Fc}/S_P, R_{Fc}$)- 3	(S_C, S_P, R_{Fc})- 4
C1–C2	1.638(5)	1.642(4)
C2–H2	0.92(3)	0.94(3)
P1–C1	1.895(3)	1.893(2)
P1–C3	1.795(3)	1.788(2)
P1–C11	2.060(2)	2.059(1)
N1···H2	2.23(3)	2.50(3)
P1–C1–C2	113.4(2)	113.7(2)
C1–P1–C3	102.4(1)	101.4(1)
C11–P1–C1	97.5(1)	97.71(8)
C11–P1–C3	100.7(1)	100.26(9)
C2–H2–N1	162(3)	143(3)

Scheme 2. Only the Formation of (S_P, S_P, R_{Fc}, R_{Fc})-5** Is Shown**



due to an intramolecular hydrogen-bonding interaction between the nitrogen atom and the slightly acidic proton of the second cage carbon atom (N1···H2 2.23(3) Å, C2–H2–N1 162(3)°). This interaction is also reflected in the NMR chemical shift of this proton. Compared to known monophosphorus-substituted *ortho*-carbaboranes, for which the corresponding signal normally appears in the region between 3 and 3.6 ppm,^{11b,c,17} in this case it is shifted downfield to 4.75 ppm.

Optically pure **4** crystallizes in the chiral space group $P2_12_12_1$, Flack parameter $x = -0.004(16)$. The structure is shown in Figure 2, and data are given in Table 1. It has similar structural features to its racemic analogue **3**. Again the amino group is involved in an intramolecular hydrogen-bonding interaction with the proton of the unsubstituted cage carbon atom (N1···H2 2.50(3) Å, C2–H2–N1 143(3)°). Due to steric interactions between the methyl group at the chiral carbon atom and the ferrocene moiety, the distance is slightly longer and the angle is smaller than in **3**, that is, further from the ideal 180°. Therefore, the ¹H NMR signal for the corresponding proton appears at slightly higher field ($\delta_H = 4.54$ ppm).

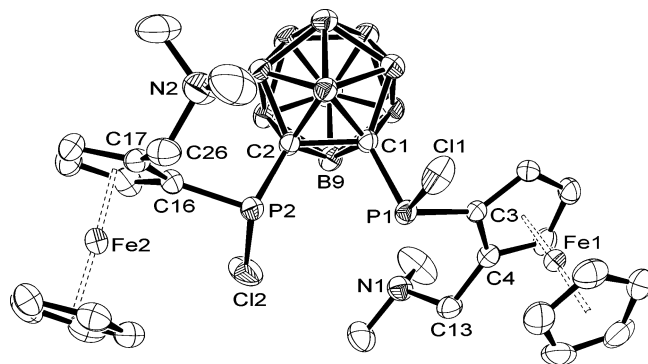


Figure 3. Molecular structure and atom-labeling scheme for the S_P, S_P, R_{Fc}, R_{Fc} enantiomer of ($R_P, R_P, S_{Fc}, S_{Fc}/S_P, S_P, R_{Fc}, R_{Fc}$)-**5** with thermal ellipsoids at the 50% probability level. H atoms are omitted for clarity.

Table 2. Selected Bond Lengths (Å) and Angles (deg) for ($R_P, R_P, S_{Fc}, S_{Fc}/S_P, S_P, R_{Fc}, R_{Fc}$)-**5**

C1–C2	1.700(2)	P2–PC	1.885(2)
P1–C1	1.891(2)	P2–C16	1.793(2)
P1–C3	1.796(2)	P2–C12	2.0652(7)
P1–C11	2.0704(7)	P2–C2–C1	115.1(1)
P1–C1–C2	114.0(1)	C2–P2–C16	100.75(8)
C1–P1–C3	100.92(7)	C12–P2–C2	99.81(6)
C11–P1–C1	98.88(6)	C12–P2–C16	99.97(6)
C11–P1–C3	100.08(6)		

To investigate whether similar stereoselectivity can be observed in the synthesis of a disubstituted carbaboranyl derivative, dilithiated 1,2-dicarba-*closo*-dodecaborane(12) was treated with 2 equiv of racemic **1** (Scheme 2). The product, 1,2-bis[chloro(2-*N,N*-dimethylaminomethylferrocenyl)phosphanyl]-1,2-dicarba-*closo*-dodecaborane(12), has two planar and two P-centered stereocenters. Therefore, the formation of eight diastereomers should be possible. Due to symmetry and like-substituted stereocenters, two pairs of them are identical and two are *meso* forms. Thus, a mixture of six diastereomers was expected. However, the ³¹P{¹H} NMR spectrum of the reaction solution showed only one major signal and traces of other products in the same region, which may belong to the other diastereomers but could not be isolated. The compound belonging to the main peak could be isolated by recrystallization of the crude product. X-ray diffraction revealed that it is the diastereomer that consists of the R_P, R_P, S_{Fc}, S_{Fc} and the S_P, S_P, R_{Fc}, R_{Fc} enantiomers. The structure of S_P, S_P, R_{Fc}, R_{Fc} -**5** is depicted in Figure 3; selected bond lengths and angles are given in Table 2. They are similar to those of the monosubstituted derivatives and of other structurally characterized symmetrically bis-chlorophosphino-substituted *ortho*-carbaboranes.^{11b,c} The NMR spectra show only one set of signals for both aminoalkylferrocenylphosphane substituents; the ¹³C{¹H} NMR spectrum displays more complex coupling patterns for all carbon atoms coupling to phosphorus due to an AA'XX' spin system. Therefore, the spectra demonstrate that the molecule adopts C_2 symmetry in solution. However, since this is not a crystallographic 2-fold axis, the two substituents are not equivalent in the solid state. The amino groups undergo neither hydrogen-bonding interactions with any of the BH groups nor any electronic interactions with the phosphorus atoms as observed for the starting material **1**.¹⁶

To explore the chemistry of the remaining chloro groups, the reactivity of ($R_P, S_{Fc}/S_P, R_{Fc}$)-**3** toward LiAlH₄ was first investigated (Scheme 3). It is known that the reactions of carbaboranylchlorophosphanes with LiAlH₄ can encounter problems,

(17) Núñez, R.; Viñas, C.; Teixidor, F.; Sillanpää, R.; Kivekäs, R. *J. Organomet. Chem.* **1999**, 592, 22.

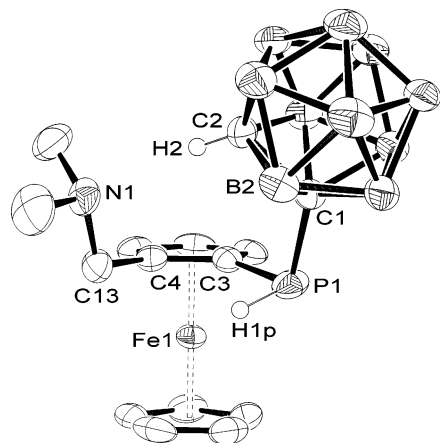


Figure 4. Molecular structure and atom-labeling scheme for the R_P,R_{FC} enantiomer of $(R_P,R_{FC}/S_P,S_{FC})$ -**6** with thermal ellipsoids at the 50% probability level. H atoms except H2 and H1p are omitted for clarity.

Scheme 3. Only the Formation of (R_P,R_{FC}) -6** Is Shown**

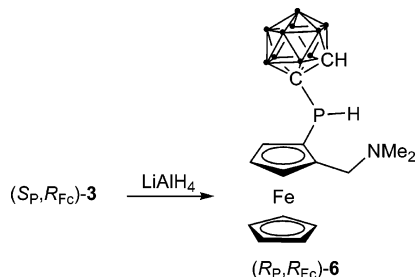


Table 3. Selected Bond Lengths (Å) and Angles (deg) for $(R_P,R_{FC}/S_P,S_{FC})$ -6****

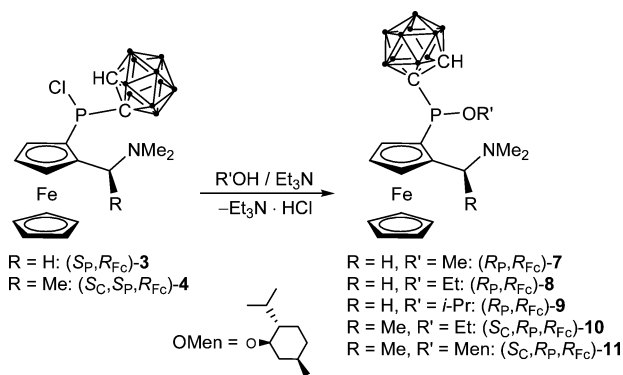
C1–C2	1.649(4)	P1–C1–C2	122.8(2)
C2–H2	0.88(3)	C1–P1–C3	105.1(1)
P1–C1	1.876(3)	C1–P1–H1p	95(1)
P1–C3	1.810(3)	C3–P1–H1p	97(1)
P1–H1p	1.33(3)	C2–H2–N1	169(3)
N1...H2	2.25(3)		

namely, cleavage of the cluster carbon–phosphorus bond.¹⁸ However, here the reaction afforded the expected product in good yield. The ³¹P NMR spectrum of the reaction mixture showed two doublets in a ratio of approximately 10:1 for the two possible diastereomers. One should show inversion at the stereogenic P center, and the second should retain the *P* chirality. The diastereomers could be separated by recrystallization, giving the major diastereomer in an overall yield of 84%. Its crystal structure is depicted in Figure 4 and reveals that it is the expected inversion product $(R_P,R_{FC}/S_P,S_{FC})$ -**6**. Selected bond lengths and angles are given in Table 3.

Compound **6** is, to the best of our knowledge, the first structurally characterized monosubstituted secondary phosphanylcarbaborane. The bond lengths and angles are within the range observed for the secondary bisphosphanylcarbaborane 1,2-bis(phenylphosphino)-1,2-dicarbaborane(12).^{18a} Therefore, $(R_P,R_{FC}/S_P,S_{FC})$ -**6** also shows slight differences of the geometry around the phosphorus atom compared to other reported bulky secondary phosphanes bearing aromatic substituents.¹⁹ The C1–P1–C3 angle is within the same range or slightly larger, while the C–P1–H angles are smaller. For most reported compounds, however, the C–P–H angles are larger than the C–P–C angle.

(18) (a) Balema, V. P.; Pink, M.; Sieler, J.; Hey-Hawkins, E.; Hennig, L. *Polyhedron* **1998**, *17*, 2087. (b) Kasantsev, A. V.; Zhubekova, M. N.; Zakharkin, L. I. *Zh. Obshch. Khim.* **1971**, *41*, 2027.

Scheme 4. Only the Reaction for the Isomer (S_P,R_{FC}) -3** Is Shown**



As for the corresponding chlorophosphane **3**, compound **6** also shows an intramolecular hydrogen-bonding interaction, which in this case is stronger. This can be deduced from the C2–H2–N1 angle, which is closer to the ideal 180° (169° vs 162°) and by the ¹H NMR chemical shift. The signal for the proton attached to the second cluster carbon atom appears about 1 ppm further downfield (5.74 vs 4.75 ppm). Compound **6** is air-stable in the solid state and did not show any oxidation after more than four weeks in solution. This lack of reactivity toward oxidation is also observed for the other two known secondary phosphanyl carbaboranes.¹⁸ Their stability is most likely due to steric bulk and the strong electron-withdrawing effect of the *ortho*-carbaborane moiety, which deactivates the phosphorus lone pair. However, **6** slowly undergoes epimerization at the phosphorus center in solution at room temperature. After 1 day, small signals appear in the NMR spectra for a second diastereomer, the same as is observed in the spectra of the crude product. After 6 months, a ratio of the two diastereomers of about 5:1 could be determined. This inversion process could be accelerated by refluxing in C₆D₆, but it still took several days to attain the 5:1 ratio, which changed only very slowly on prolonged heating.

To further study the reactivity of the carbaboranylchlorophosphanes toward substitution of the chloro groups, they were treated with alcohols in the presence of a base (Scheme 4). Thus, an excess of triethylamine and the alcohol, which also served as solvent, were added to solid $(R_P,S_{FC}/S_P,R_{FC})$ -**3**. Methanol, ethanol, and 2-propanol were used and displayed very similar reactivities. The reactions occurred at room temperature and were complete after stirring overnight. ³¹P{¹H} NMR spectra of the reaction mixtures showed the exclusive formation of only one diastereomer in each case; a second diastereomer could never be detected. The products $(R_P,R_{FC}/S_P,S_{FC})$ -**7**, $(R_P,R_{FC}/S_P,S_{FC})$ -**8**, and $(R_P,R_{FC}/S_P,S_{FC})$ -**9** could be recrystallized and isolated as crystalline solids in excellent yields. An increase of solubility in *n*-hexane from **7** to **9** could be observed. While **7** is only poorly soluble, **8** is readily soluble in hot *n*-hexane, and **9** was too soluble for recrystallization from this solvent. Therefore, *n*-pentane had to be used. The configurations of the stereocenters were confirmed by X-ray analyses, which revealed that the three new compounds are the expected products with inverted stereochemistry at the phosphorus atom with respect to the starting material $(R_P,S_{FC}/S_P,R_{FC})$ -**3**. Their crystal structures are

(19) (a) Bartlett, R. A.; Olmstead, M. M.; Power, P. P.; Sigel, G. A. *Inorg. Chem.* **1987**, *26*, 1941. (b) Wicht, D. K.; Kovacic, I.; Glueck, D. S.; Liabile-Sands, L. M.; Incarvito, C. D.; Rheingold, A. L. *Organometallics* **1999**, *18*, 5141. (c) Koch, T.; Blaurock, S.; Somoza, F., Jr.; Hey-Hawkins, E. *Eur. J. Inorg. Chem.* **2000**, 2167. (d) Höcher, T.; Blaurock, S.; Hey-Hawkins, E. *Eur. J. Inorg. Chem.* **2002**, 1174.

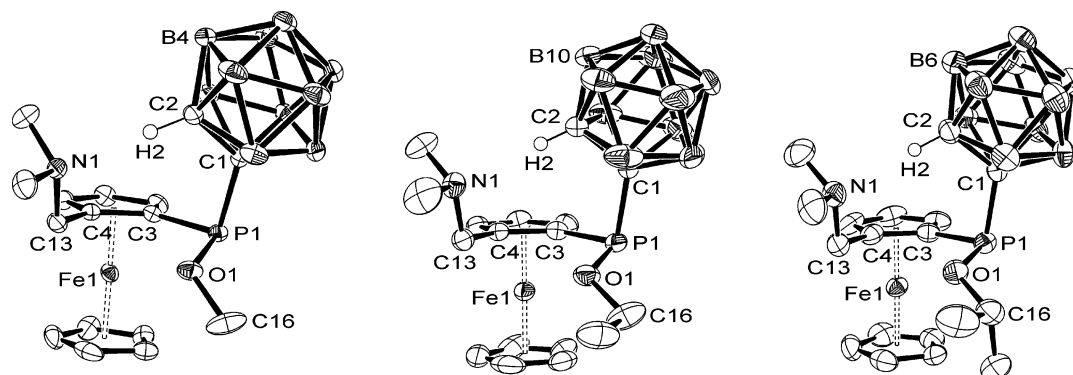


Figure 5. Molecular structures and atom-labeling schemes for the R_P,R_{Fc} enantiomers of $(R_P,R_{Fc}/S_P,S_{Fc})$ -7, $(R_P,R_{Fc}/S_P,S_{Fc})$ -8, and $(R_P,R_{Fc}/S_P,S_{Fc})$ -9 with thermal ellipsoids at the 50% probability level. H atoms except H2 are omitted for clarity. For **8**, only one of two crystallographically independent molecules present in the asymmetric unit is shown.

Table 4. Selected Bond Lengths (Å) and Angles (deg) for $(R_P,R_{Fc}/S_P,S_{Fc})$ -7, $(R_P,R_{Fc}/S_P,S_{Fc})$ -8, $(R_P,R_{Fc}/S_P,S_{Fc})$ -9, (S_C,R_P,R_{Fc}) -10, and (S_C,R_P,R_{Fc}) -11

	$(R_P,R_{Fc}/S_P,S_{Fc})$ -7	$(R_P,R_{Fc}/S_P,S_{Fc})$ -8	$(R_P,R_{Fc}/S_P,S_{Fc})$ -9	(S_C,R_P,R_{Fc}) -10	(S_C,R_P,R_{Fc}) -11
C1–C2	1.642(2)	1.635(4)	1.652(2)	1.644(2)	1.644(2)
C2–H2	0.98(2)	0.92(4)	0.94(2)	0.99(2)	0.90(2)
P1–C1	1.886(1)	1.889(2)	1.895(2)	1.883(2)	1.898(1)
P1–C3	1.793(1)	1.795(3)	1.800(2)	1.800(2)	1.798(1)
P1–O1	1.628(1)	1.625(2)	1.633(1)	1.629(1)	1.6364(8)
O1–C16(C17) ^a	1.437(2)	1.458(4)	1.467(2)	1.46(1)	1.468(1)
N1···H2	2.13(2)	2.21(4)	2.20(2)	2.21(3)	2.28(2)
P1–C1–C2	124.54(9)	124.2(2)	123.7(1)	123.5(1)	124.88(8)
C1–P1–C3	101.75(6)	101.6(1)	100.70(8)	101.64(7)	100.03(5)
O1–P1–C1	100.39(6)	100.2(1)	101.16(7)	100.28(7)	103.02(5)
O1–P1–C3	100.77(6)	100.7(1)	100.59(8)	101.61(7)	102.33(5)
P1–O1–C16(C17) ^a	116.9(1)	115.2(2)	118.2(1)	116.0(6)	118.47(7)
C2–H2–N1	173(2)	179(4)	169(2)	159(2)	161(2)

^a Distance or angle refers to C16 for $(R_P,R_{Fc}/S_P,S_{Fc})$ -7, $(R_P,R_{Fc}/S_P,S_{Fc})$ -8, and $(R_P,R_{Fc}/S_P,S_{Fc})$ -9, and to C17 for (S_C,R_P,R_{Fc}) -10 and (S_C,R_P,R_{Fc}) -11.

shown in Figure 5; selected bond lengths and angles are given in Table 4. The *P*-chiral compounds $(R_P,R_{Fc}/S_P,S_{Fc})$ -7, $(R_P,R_{Fc}/S_P,S_{Fc})$ -8, and $(R_P,R_{Fc}/S_P,S_{Fc})$ -9 are the first phosphinites with both ferrocenyl and carbaboranyl substituents at phosphorus. The geometries around the phosphorus centers display no significant changes with increasing steric demand of the alkoxy substituents and are comparable to those of other structurally characterized phosphinites with aromatic and bulky substituents.²⁰ The P–C and P–O bond lengths are within the same range; the C–P–C and O–P–C bond angles are slightly smaller. The characteristic intramolecular hydrogen bond between the nitrogen atom of the dimethylamino group and the proton of the second cluster carbon atom is, similar to $(R_P,R_{Fc}/S_P,S_{Fc})$ -6, stronger than in the corresponding starting material $(R_P,S_{Fc}/S_P,R_{Fc})$ -3. The N1···H2 distances are shorter (between 2.13 and 2.21 Å) and the C2–H2–N1 angles closer to the ideal 180° (between 169° and 179°). The ¹H NMR chemical shifts of these protons are close to 6 ppm.

Compounds $(R_P,R_{Fc}/S_P,S_{Fc})$ -7, $(R_P,R_{Fc}/S_P,S_{Fc})$ -8, and $(R_P,R_{Fc}/S_P,S_{Fc})$ -9 are completely stable toward oxygen and water both in the solid state and in solution. The *P*-stereogenic centers of these carbaboranylferrocenyl phosphinites are, in contrast to the secondary phosphane $(R_P,R_{Fc}/S_P,S_{Fc})$ -6, very stable toward inversion and therefore epimerization. After refluxing in toluene under air for 48 h, no trace of a second diastereomer could be

detected. Also, migration of the alkyl groups from oxygen to phosphorus to form phosphane oxides or any other oxidation could not be observed. This chemical stability of *ortho*-carbaborane-substituted phosphanes is well-known.²¹ Due to the strongly electron-withdrawing effect of the *ortho*-carbaborane cluster, the lone pair of the phosphorus atom is deactivated. Therefore, its trivalent state is exceptionally stabilized.

Given the inversion of the *P* chirality on substitution of the chloro group of $(R_P,S_{Fc}/S_P,R_{Fc})$ -3 by alkoxides, the same synthetic strategy was applied to obtain an enantiopure derivative. Thus, optically pure chlorophosphane (S_C,S_P,R_{Fc}) -4 was treated with ethanol in the presence of triethylamine to afford (S_C,R_P,R_{Fc}) -10, the enantiomerically pure analogue of $(R_P,R_{Fc}/S_P,S_{Fc})$ -8. The reactivity was identical, and again substitution of the chloro group was 100% stereoselective. The product was characterized by X-ray diffraction. The structure in the solid state is displayed in Figure 6, and selected data are given in Table 4. It is very similar to that of (R_P,R_{Fc}) -8. The only significant difference is caused by the methyl group of the chiral carbon center in the aminoalkyl side chain of the substituted Cp ring. As is also observed for (S_C,S_P,R_{Fc}) -4, steric interactions between this methyl group and the ferrocene moiety force the dimethylamino group into a position where the C2–H2–N1 angle is smaller, that is, further away from the ideal 180°.

For the synthesis of an enantiopure carbaboranylferrocenyl phosphinite with a bulky alkoxy group, (–)-menthol was chosen. It was used in 3-fold excess together with triethylamine

(20) (a) Bayersdörfer, R.; Ganter, B.; Englert, U.; Keim, W.; Vogt, D. *J. Organomet. Chem.* **1998**, 552, 187. (b) Brunet, J.-J.; Chauvin, R.; Chiffre, J.; Donnadiou, B.; Huguet, S.; Leglaye, P.; Mothes, E. *Inorg. Chim. Acta* **1999**, 291, 300. (c) Nazarov, A. A.; Hartinger, C. G.; Arion, V. B.; Giester, G.; Keppler, B. K. *Tetrahedron* **2002**, 58, 8489.

(21) Núñez, R.; Viñas, C.; Teixidor, F.; Sillanpää, R.; Kivekäs, R. *J. Organomet. Chem.* **1999**, 592, 22.

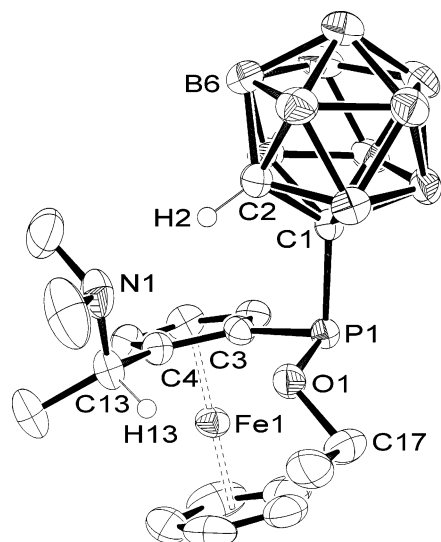


Figure 6. Molecular structure and atom-labeling scheme for (S_C, R_P, R_{Fc})-**10** with thermal ellipsoids at the 50% probability level. One part of the disordered ethyl group and H atoms except H2 and H13 are omitted for clarity.

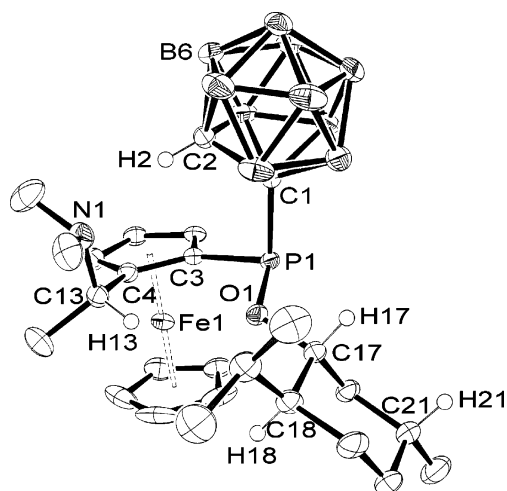


Figure 7. Molecular structure and atom-labeling scheme of (S_C, R_P, R_{Fc})-**11** with thermal ellipsoids at the 50% probability level. H atoms except H2 and those at chiral centers are omitted for clarity.

dissolved in diethyl ether. The chlorophosphane starting material (S_C, S_P, R_{Fc})-**4** was added as a solid. The reaction went to completion at room temperature overnight and was again found to be 100% stereoselective. The menthol-substituted phosphinite (S_C, R_P, R_{Fc})-**11** was recrystallized from *n*-pentane and isolated in excellent yield as a single enantiomer, as was also confirmed by X-ray analysis. The solid-state structure is depicted in Figure 7; selected bond lengths and angles are given in Table 4. The structural features are very similar to those of (S_C, R_P, R_{Fc})-**10**; the O–P–C and P–O–C bond angles are slightly larger due to the greater steric demand of the menthyl group. The other enantiomers of (S_C, R_P, R_{Fc})-**10** and (S_C, R_P, R_{Fc})-**11** ((R_C, S_P, S_{Fc}) -**10** and (R_C, S_P, S_{Fc}) -**11**) were obtained by using (R_C, R_P, S_{Fc}) -**4** as starting material instead of (S_C, S_P, R_{Fc})-**4**.

Comparison of the arrangements of coordinating groups of the carbaboranylferrocenylchlorophosphanes and the carbaboranylferrocenyl phosphinites reveals one major difference. In the structures of $(R_P, S_{Fc}/S_P, R_{Fc})$ -**3** and (S_C, S_P, R_{Fc}) -**4** the electron lone pairs of the nitrogen atom and of the phosphorus atom are directed in such a way that the two donor groups can chelate a metal center. Substitution of the chloro groups inverted the

configurations of the phosphorus centers. Therefore, the electron lone pairs of the phosphorus atoms of all presented phosphinites are pointed in the opposite direction to the nitrogen lone pairs. Thus, to chelate metal centers, the ligand molecules have to rearrange in such a way that the carbaborane and the ferrocene moieties are forced into close proximity, causing steric strain and hemilability with interesting possibilities for homogeneous catalysis.

Conclusions

Novel *P*-chiral carbaboranylferrocenylchlorophosphanes, a secondary carbaboranylferrocenylphosphane, and carbaboranylferrocenyl phosphinites were synthesized and fully characterized. The absolute configurations of the stereogenic centers were determined by X-ray diffraction in every case. The chloro groups of the starting materials **1** and **2** can subsequently be substituted diastereoselectively, leading to diastereomerically pure compounds in the case of **1** and to enantiomerically pure compounds in the case of homochiral **2**. As substituent, the strongly electron-withdrawing 1,2-dicarba-*closo*-dodecaboran(12)yl group was first chosen, which changes the coordinating abilities of the phosphorus donor atom, stabilizes its trivalent state, and thus protects it from oxidation. The *ortho*-carbaborane can also be difunctionalized with high stereoselectivity to introduce two ferrocenylchlorophosphanyl groups. However, in all monosubstituted *ortho*-carbaboranes, the proton of the second cluster carbon atom was found to undergo intramolecular hydrogen-bonding interaction with the nitrogen atom of the dimethylamino group in the ferrocenyl unit. The second chloro group of the corresponding starting material was replaced by either a hydride or alkoxides. The latter substitution showed 100% stereoselectivity, that is, complete inversion at the phosphorus center with respect to the carbaboranylferrocenylchlorophosphanes. The synthesized phosphinite ligands show interesting geometrical features, which offer opportunities to use them as hemilabile bidentate ligands in metal complexes. The coordinating properties of the presented ligands and the catalytic activities of the resulting complexes are the subject of further investigations.

Experimental

General Considerations. All manipulations were carried out using standard Schlenk techniques under an atmosphere of dry high-purity nitrogen. Diethyl ether, toluene, and *n*-hexane were taken from an MBraun solvent purification system MB SPS-800; *n*-pentane was distilled from sodium. All these solvents were nitrogen-saturated and stored over potassium mirror. Methanol, ethanol, and 2-propanol were degassed in a nitrogen stream in an ultrasonic bath. Starting materials **1** and enantiomerically pure **2** were synthesized according to the procedures previously reported by us.¹⁶ Other chemicals were obtained from commercial sources and used as supplied. ¹H (400.13 MHz), ¹¹B (128.38 MHz), ¹³C (100.16 MHz), and ³¹P (161.98 MHz) NMR spectra were recorded on a Bruker Avance DRX 400 spectrometer at +20 °C in C₆D₆ and referenced to tetramethylsilane (TMS).²² Mass spectra were recorded on a VG Analytics ZAB-HSQ spectrometer (EI pos. 70 eV). FT-IR spectra were recorded on a Perkin-Elmer Spectrum 2000 spectrometer in KBr. Melting points were determined in sealed glass capillaries under nitrogen and are uncorrected. The described synthetic procedures for enantiomerically pure compounds are fully applicable to afford the corresponding second enantiomers by using the other enantiomers of the starting materials.

(22) Harris, R. K.; Becker, E. D.; Cabral de Menezes, S. M.; Goodfellow, R.; Granger, P. *Pure Appl. Chem.* **2001**, *73*, 1795.

1-[1-(1,2-Dicarba-closo-dodecaboran(12)yl)chlorophosphanyl]-2-*N,N*-dimethylaminomethylferrocene ((*R_P*,*S_{FC}*/*S_P*,*R_{FC}*)-3). To a solution of 1,2-dicarba-closo-dodecaborane(12) (0.42 g, 2.91 mmol) in toluene (10 mL) at 0 °C was slowly added *n*-BuLi (1.2 mL, 2.87 mmol, 2.39 M in *n*-hexane). The resulting suspension was stirred at 0 °C for 30 min and at room temperature for 2 h. It was then slowly transferred to a cold (−50 °C) solution of *rac*-1 (1.00 g, 2.91 mmol) in toluene (20 mL). The mixture was warmed to room temperature overnight and filtered. The solvent was evaporated, and the dried residue was recrystallized from a mixture of toluene (1 mL) and *n*-hexane (20 mL) and stored at −18 °C. Crystals suitable for X-ray diffraction were grown from the same mixture at room temperature. Yield: 1.07 g (83% based on *n*-BuLi). Mp: 148–149 °C. ¹H NMR: δ 1.73 (s, 6H, NMe₂), 1.82–3.68 (m, v br, 10H, B₁₀H₁₀), 2.29 (d, ²J_{HH} = 12.8 Hz, 1H, CH₂N), 3.31 (d, ²J_{HH} = 12.8 Hz, 1H, CH₂N), 3.86 (s, 6H, Cp and 1H of C₅H₃), 4.00 (s, 1H, C₅H₃), 4.24 (s, 1H, C₅H₃ *o* to P), 4.75 (s, br, 1H, C_{Cluster}H). ¹³C{¹H} NMR: δ 44.1 (NMe₂), 57.5 (d, ³J_{PC} = 8.9 Hz, CH₂N), 60.2 (d, ²J_{PC} = 8.1 Hz, C_{Cluster}H), 70.3 (C₅H₃), 70.7 (Cp), 71.5 (C₅H₃), 74.7 (d, ²J_{PC} = 4.0 Hz, C₅H₃ *o* to P), 74.9 (d, ¹J_{PC} = 95.4 Hz, C_{Cluster}P), 75.9 (d, ¹J_{PC} = 37.5 Hz, C_{FC}P), 92.7 (d, ²J_{PC} = 31.1 Hz, C_{FC}CH₂N). ³¹P{¹H} NMR: δ 92.4. ¹¹B{¹H} NMR: δ −11.7 (s, br, 6B), −8.2 (s, br, 2B), −0.5 (s, br, 2B). FT-IR (cm^{−1}): ν_{BH} 2591 (vs). MS (*m/z*): 453 [(M + H)⁺] (16.8%), 416 [(M − Cl)⁺] (2.6%), 408 [(M − NMe₂)⁺] (2.2%), 308 [(M − C₂B₁₀H₁₁)⁺] (8.0%), 295 [(M − Cp − Fe − Cl)⁺] (10.4%), 242 [(FeCH₂NMe₂ − H)⁺] (11.0%), 152 [(C₅H₃-1-P-2-CH₂NMe₂)⁺] (100%), 109 [(C₅H₃-1-P-2-CH₂ + H)⁺] (32.1%), 58 [(CH₂=NMe₂)⁺] (42.0%). Anal. Calcd for C₁₅H₂₇B₁₀ClFeNP: C, 39.88; H, 6.01; N, 3.10. Found: C, 40.02; H, 5.93; N, 2.99.

(*S*)-*N,N*-Dimethyl-1-[(*R*)-2-[(*S*)-{1-(1,2-dicarba-closo-dodecaboran(12)yl)chlorophosphanyl}ferrocenyl]ethylamine ((*S_C*,*S_P*,*R_{FC}*)-4). The same procedure as for the synthesis and recrystallization of **3** was followed using 1,2-dicarba-closo-dodecaborane(12) (0.39 g, 2.70 mmol), *n*-BuLi (1.1 mL, 2.63 mmol, 2.39 M in *n*-hexane), and (*S,R*)-2 (1.00 g, 2.79 mmol). Yield: 0.96 g (78% based on *n*-BuLi). Mp: 164–165 °C. ¹H NMR: δ 0.80 (d, ³J_{HH} = 6.4 Hz, 3H, CH−CH₃), 1.68 (s, 6H, NMe₂), 1.72–3.55 (m, v br, 10H, B₁₀H₁₀), 3.56 (q, ³J_{HH} = 6.4 Hz, 1H, CH−Me), 3.86 (s, 5H, Cp), 3.92 (s, 1H, C₅H₃), 4.03 (s, 1H, C₅H₃), 4.28 (s, 1H, C₅H₃ *o* to P), 4.54 (s, br, 1H, C_{Cluster}H). ¹³C{¹H} NMR: δ 7.1 (CH−CH₃), 38.7 (NMe₂), 56.9 (d, ³J_{PC} = 9.0 Hz, CH−Me), 60.0 (d, ²J_{PC} = 7.5 Hz, C_{Cluster}H), 70.3 (C₅H₃), 70.8 (d, ²J_{PC} = 4.2 Hz, C₅H₃ *o* to P), 70.9 (Cp), 71.2 (C₅H₃), 75.0 (d, ¹J_{PC} = 96.1 Hz, C_{Cluster}P), 76.1 (d, ¹J_{PC} = 39.4 Hz, C_{FC}P), 99.4 (d, ²J_{PC} = 32.2 Hz, C_{FC}CHN). ³¹P{¹H} NMR: δ 93.4. ¹¹B{¹H} NMR: δ −11.6 (s, br, 6B), −8.3 (s, br, 2B), −0.7 (s, br, 2B). FT-IR (cm^{−1}): ν_{BH} 2574 (vs). MS (*m/z*): 466 [M⁺] (13.2%), 421 [(M − HNMe₂)⁺] (3.6%), 402 [(M − Cp + H)⁺] (8.9%), 212 [(FeCH=CH₂)⁺] (8.5%), 166 [(C₅H₃-1-P-2-CH(Me)NMe₂)⁺] (53.9%), 72 [(MeCH=NMe₂)⁺] (100%). Anal. Calcd for C₁₆H₂₉B₁₀ClFeNP: C, 41.28; H, 6.28; N, 3.01. Found: C, 41.58; H, 6.01; N, 2.87.

1,2-Bis[chloro(2-*N,N*-dimethylaminomethylferrocenyl)phosphanyl]-1,2-dicarba-closo-dodecaborane(12) ((*R_P*,*R_P*,*S_{FC}*,*S_{FC}*/*S_P*,*S_P*,*R_{FC}*,*R_{FC}*)-5). To a solution of 1,2-dicarba-closo-dodecaborane(12) (0.25 g, 1.73 mmol) in diethyl ether (15 mL) at 0 °C was slowly added *n*-BuLi (1.45 mL, 3.47 mmol, 2.39 M in *n*-hexane). The resulting suspension was stirred at 0 °C for 30 min and at room temperature for an additional 2 h. It was then slowly transferred to a cold (−80 °C) suspension of *rac*-1 (1.20 g, 3.50 mmol) in toluene (15 mL). The resulting mixture was slowly warmed to room temperature and stirred overnight. It was then filtered, and the solvent was removed in vacuo. The dried residue was recrystallized from a mixture of toluene (2 mL) and *n*-hexane (20 mL). Brown crystals formed at −18 °C over a few days. They were isolated, washed with *n*-hexane, and dried in vacuo. Yield: 0.69 g (53% based on 1,2-dicarba-closo-dodecaborane(12)). Mp:

195 °C (dec). ¹H NMR: δ 1.90–3.83 (m, v br, 10H, B₁₀H₁₀), 2.18 (s, 12H, NMe₂), 2.74 (d, ²J_{HH} = 12.8 Hz, 2H, CH₂N), 3.73 (d, ²J_{HH} = 12.8 Hz, 2H, CH₂N), 3.96 (s, 10H, Cp), 4.00 (s, 4H, all C₅H₃ *m* to P), 4.52 (s, 2H, C₅H₃ *o* to P). ¹³C{¹H} NMR: δ 45.0 (NMe₂), 58.3 (m, CH₂N), 71.0 (Cp), 71.1 (C₅H₃), 71.7 (C₅H₃), 74.0 (br, C₅H₃ *o* to P), 77.2 (m, C_{FC}P), 84.4 (m, C_{Cluster}), 93.8 (m, C_{FC}−CH₂N). ³¹P{¹H} NMR: δ 87.0. ¹¹B{¹H} NMR: δ −9.2 (s, br, 4B), −7.1 (s, br, 4B), −0.2 (s, br, 2B). FT-IR (cm^{−1}): ν_{BH} 2570 (vs). MS (*m/z*): 760 [(M + H)⁺] (1.6%), 687 [(M − 2Cl − H)⁺] (1.3%), 459 [(M − 2Cl − 2Cp − Fe − NMe₂)⁺] (2.8%), 452 [(M − 1-PCl − 2-CH₂NMe₂ − C₅H₃FeCp + H)⁺] (3.9%), 415 [(M − 1-PCl − 2-CH₂−NMe₂−C₅H₃FeCp − Cl)⁺] (4.8%), 152 [(1-P-2-CH₂NMe₂−C₅H₃)⁺] (23.6%), 66 [(CpH)⁺] (100%). Anal. Calcd for C₂₈H₄₂B₁₀Cl₂−Fe₂N₂P₂: C, 44.29; H, 5.58; N, 3.69. Found: C, 44.34; H, 5.41; N, 3.45.

1-[1-(1,2-Dicarba-closo-dodecaboran(12)yl)phosphanyl]-2-*N,N*-dimethylaminomethylferrocene ((*R_P*,*R_{FC}*/*S_P*,*S_{FC}*)-6). To a suspension of LiAlH₄ (0.02 g, 0.53 mmol) in diethyl ether (15 mL) at −80 °C was added solid (*R_P*,*S_{FC}*/*S_P*,*R_{FC}*)-3 (0.50 g, 1.11 mmol) in one portion. The yellow mixture was warmed to room temperature and stirred for a further hour. After cooling to 0 °C, water (10 mL) was slowly added and the resulting mixture was stirred for 2 h at room temperature. The phases were separated, and the aqueous layer was washed with diethyl ether (5 mL). The combined organic phases were dried over MgSO₄, filtered, and reduced in vacuo to about one-third of their volume. At −18 °C light yellow crystals grew over a few days, which were isolated by filtration, washed with a small amount of cold diethyl ether, and dried in vacuo. Yield: 0.39 g (84%). Mp: 153–154 °C. ¹H NMR: δ 1.78 (s, 6H, NMe₂), 1.92–3.65 (m, v br, 10H, B₁₀H₁₀), 2.21 (d, ²J_{HH} = 12.0 Hz, 1H, CH₂N), 3.02 (d, ²J_{HH} = 12.0 Hz, 1H, CH₂N), 3.74 (s, 5H, Cp), 3.88 (s, 1H, C₅H₃ *o* to CH₂N), 3.97 (m, 1H, C₅H₃ *m* to P and *m* to CH₂N), 4.10 (m, 1H, C₅H₃ *o* to P), 4.84 (d, ¹J_{PH} = 228.0 Hz, 1H, PH), 5.74 (s, br, 1H, C_{Cluster}H). ¹³C{¹H} NMR: δ 44.1 (NMe₂), 57.2 (CH₂N), 63.8 (d, ²J_{PC} = 3.1 Hz, C_{Cluster}H), 68.1 (d, ¹J_{PC} = 14.3 Hz, C_{FC}P), 69.9 (Cp), 70.1 (d, ¹J_{PC} = 74.2 Hz, C_{Cluster}P), 71.8 (d, ³J_{PC} = 9.8 Hz, C₅H₃ *m* to P and *m* to CH₂N), 75.0 (C₅H₃ *o* to CH₂N), 78.8 (d, ²J_{PC} = 39.9 Hz, C₅H₃ *o* to P), 86.2 (d, ²J_{PC} = 6.7 Hz, C_{FC}CH₂N). ³¹P NMR: δ −36.1 (d, ¹J_{PH} = 228.0 Hz). ¹¹B{¹H} NMR: δ −12.4 (s, br, 1B), −11.0 (s, br, 3B), −9.7 (s, br, 2B), −8.3 (s, br, 2B), −2.4 (s, br, 1B), 0.4 (s, br, 1B). FT-IR (cm^{−1}): ν_{BH} 2581 (vs), ν_{PH} 2331 (m). MS (*m/z*): 417 [M⁺] (9.8%), 372 [(M − HNMe₂)⁺] (100%), 305 [(M − Cp − HNMe₂ − 2H)⁺] (11.1%), 292 [(M − Cp − NMe₃ − H)⁺] (10.4%), 121 [(FeCp)⁺] (48.2%), 58 [(CH₂=NMe₂)⁺] (28.9%). Anal. Calcd for C₁₅H₂₈B₁₀−FeNP: C, 43.17; H, 6.76; N, 3.36. Found: C, 43.31; H, 6.54; N, 3.21.

1-[1-(1,2-Dicarba-closo-dodecaboran(12)yl)methoxyphosphanyl]-2-*N,N*-dimethylaminomethylferrocene ((*R_P*,*R_{FC}*/*S_P*,*S_{FC}*)-7). To (*R_P*,*S_{FC}*/*S_P*,*R_{FC}*)-3 (0.5 g, 1.11 mmol) were added successively triethylamine (3.0 mL) and methanol (20 mL). After stirring at room temperature overnight all volatile substances were removed in vacuo and the dried residue was extracted with five 20 mL portions of hot *n*-hexane. The volume of the solution was reduced slightly in vacuo and kept at −18 °C. Orange crystals formed within a few days, which were isolated, washed with *n*-hexane, and dried in vacuo. Yield: 0.49 g (99%). Mp: 197–198 °C. ¹H NMR: δ 1.85 (s, 6H, NMe₂), 1.80–3.65 (m, v br, 10H, B₁₀H₁₀), 2.26 (d, ²J_{HH} = 12.0 Hz, 1H, CH₂N), 3.32 (d, ³J_{PH} = 14.0 Hz, 3H, POMe), 3.60 (d, ²J_{HH} = 12.0 Hz, 1H, CH₂N), 3.87 (s, 1H, C₅H₃ *o* to CH₂N), 3.91 (s, 5H, Cp), 3.95 (m, 1H, C₅H₃ *m* to P and *m* to CH₂N), 4.07 (m, 1H, C₅H₃ *o* to P), 5.91 (s, br, 1H, C_{Cluster}H). ¹³C{¹H} NMR: δ 44.3 (NMe₂), 57.8 (CH₂N), 59.6 (d, ²J_{PC} = 27.9 Hz, POMe), 61.4 (C_{Cluster}H), 69.9 (Cp), 71.5 (d, ³J_{PC} = 12.4 Hz, C₅H₃ *m* to P and *m* to CH₂N), 75.3 (d, ¹J_{PC} = 14.4 Hz, C_{FC}P), 75.6 (C₅H₃ *o* to CH₂N), 76.2 (d, ²J_{PC} = 51.1 Hz, C₅H₃ *o* to P), 77.8 (d, ¹J_{PC} = 94.6 Hz, C_{Cluster}P), 85.7 (d, ²J_{PC} = 4.1 Hz, C_{FC}CH₂N). ³¹P-

{¹H} NMR: δ 146.5. ¹¹B{¹H} NMR: δ -11.1 (s, br, 6B), -9.0 (s, br, 1B), -8.3 (s, br, 1B), -1.2 (s, br, 1B), 0.1 (s, br, 1B). FT-IR (cm⁻¹): ν_{BH} 2580 (vs). MS (EI pos. 10 eV, *m/z*): 447 [M⁺] (100%), 432 [(M - Me)⁺] (6.6%), 403 [(M - NMe₂)⁺] (11.4%), 304 [(M - C₂B₁₀H₁₁)⁺] (49.7%), 242 [(FcCH₂NMe₂ - H)⁺] (26.4%), 143 [(C₂B₁₀H₁₁)⁺] (7.8%), 66 [(CpH)⁺] (7.5%). Anal. Calcd for C₁₆H₃₀B₁₀FeNOP: C, 42.96; H, 6.76; N, 3.13. Found: C, 42.88; H, 6.81; N, 2.98.

1-[1-(1,2-Dicarba-closo-dodecaboran(12)yl)ethoxyphosphanyl]-2-*N,N*-dimethylaminomethylferrocene ((R_P,R_{FC}/S_P,S_{FC})-8). The same procedure as for the synthesis and recrystallization of (R_P,R_{FC}/S_P,S_{FC})-7 was applied with the same amounts of starting materials but with ethanol (20 mL) instead of methanol as solvent. The *n*-hexane extract of the dried reaction mixture was reduced in vacuo to about 50% and kept at -18 °C. To increase the yield, the mother liquor was again reduced in vacuo after recrystallization. Yield: 0.49 g (96%). Mp: 130–131 °C. ¹H NMR: δ 1.00 (t, ³J_{HH} = 7.0 Hz, 3H, OCH₂CH₃), 1.87 (s, 6H, NMe₂), 1.54–3.82 (m, v br, 10H, B₁₀H₁₀), 2.27 (d, ²J_{HH} = 12.4 Hz, 1H, CH₂N), 3.59 (m, 1H, OCH₂), 3.69 (d, ²J_{HH} = 12.4 Hz, 1H, CH₂N), 3.73 (m, 1H, OCH₂), 3.89 (s, 1H, C₅H₃ *o* to CH₂N), 3.92 (s, 5H, Cp), 3.97 (m, 1H, C₅H₃ *m* to P and *m* to CH₂N), 4.09 (m, 1H, C₅H₃ *o* to P), 5.91 (s, br, 1H, C_{Cluster}H). ¹³C{¹H} NMR: δ 16.8 (d, ³J_{PC} = 9.4 Hz, OCH₂CH₃), 44.2 (NMe₂), 57.8 (CH₂N), 61.3 (C_{Cluster}H), 68.7 (d, ²J_{PC} = 26.4 Hz, POCH₂), 69.9 (Cp), 71.3 (d, ³J_{PC} = 12.1 Hz, C₅H₃ *m* to P and *m* to CH₂N), 75.5 (C₅H₃ *o* to CH₂N), 75.7 (d, ¹J_{PC} = 14.3 Hz, C_{FC}P), 76.0 (d, ²J_{PC} = 50.1 Hz, C₅H₃ *o* to P), 78.1 (d, ¹J_{PC} = 95.6 Hz, C_{Cluster}P), 85.5 (d, ²J_{PC} = 4.1 Hz, C_{FC}CH₂N). ³¹P{¹H} NMR: δ 140.8. ¹¹B{¹H} NMR: δ -11.3 (s, br, 6B), -9.0 (s, br, 1B), -8.4 (s, br, 1B), -1.3 (s, br, 1B), -0.1 (s, br, 1B). FT-IR (cm⁻¹): ν_{BH} 2625 (m), 2579 (vs). MS (EI pos. 14 eV, *m/z*): 461 [M⁺] (100%), 446 [(M - Me)⁺] (4.3%), 432 [(M - Et)⁺] (8.5%), 417 [(M - NMe₂)⁺] (6.4%), 318 [(M - C₂B₁₀H₁₁)⁺] (61.0%), 275 [(M - NMe₂ - C₂B₁₀H₁₁ + H)⁺] (19.7%), 242 [(FcCH₂NMe₂ - H)⁺] (42.5%). Anal. Calcd for C₁₇H₃₂B₁₀FeNOP: C, 44.26; H, 6.99; N, 3.04. Found: C, 44.08; H, 6.99; N, 2.98.

1-[1-(1,2-Dicarba-closo-dodecaboran(12)yl)isopropoxyphosphanyl]-2-*N,N*-dimethylaminomethylferrocene ((R_P,R_{FC}/S_P,S_{FC})-9). The procedure for the synthesis of (R_P,R_{FC}/S_P,S_{FC})-7 was applied

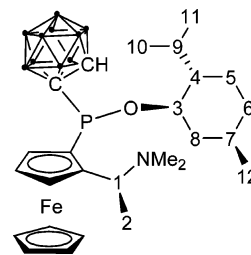


Figure 8. Assignment scheme for (S_C,R_P,R_{FC})-11.

with the same amount of (R_P,S_{FC}/S_P,R_{FC})-3 and triethylamine but with 2-propanol (20 mL) as solvent. Due to the higher solubility of the product, *n*-pentane was used for extraction and recrystallization. Yield: 0.47 g (89%). Mp: 136–137 °C. ¹H NMR: δ 1.10 (d, ³J_{HH} = 6.0 Hz, 3H, OCHCH₃), 1.11 (d, ³J_{HH} = 6.0 Hz, 3H, OCHCH₃), 1.88 (s, 6H, NMe₂), 1.74–3.65 (m, v br, 10H, B₁₀H₁₀), 2.27 (d, ²J_{HH} = 12.4 Hz, 1H, CH₂N), 3.71 (d, ²J_{HH} = 12.4 Hz, 1H, CH₂N), 3.93 (s, 1H, C₅H₃ *o* to CH₂N), 3.95 (s, 5H, Cp), 3.96 (m, 1H, OCH), 3.97 (m, 1H, C₅H₃ *m* to P and *m* to CH₂N), 4.09 (m, 1H, C₅H₃ *o* to P), 5.85 (s, br, 1H, C_{Cluster}H). ¹³C{¹H} NMR: δ 23.4 (d, ³J_{PC} = 7.2 Hz, OCHCH₃), 23.9 (d, ³J_{PC} = 5.6 Hz, OCHCH₃), 44.2 (NMe₂), 57.7 (CH₂N), 61.1 (C_{Cluster}H), 69.9 (Cp), 71.0 (d, ³J_{PC} = 11.7 Hz, C₅H₃ *m* to P and *m* to CH₂N), 74.7 (d, ²J_{PC} = 21.4 Hz, POCH), 75.5 (C₅H₃ *o* to CH₂N), 75.8 (d, ²J_{PC} = 49.8 Hz, C₅H₃ *o* to P), 76.8 (d, ¹J_{PC} = 15.8 Hz, C_{FC}P), 78.4 (d, ¹J_{PC} = 97.6 Hz, C_{Cluster}P), 85.3 (d, ²J_{PC} = 4.1 Hz, C_{FC}CH₂N). ³¹P{¹H} NMR: δ 133.0. ¹¹B{¹H} NMR: δ -11.3 (s, br, 6B), -9.0 (s, br, 1B), -8.6 (s, br, 1B), -1.2 (s, br, 1B), 0.1 (s, br, 1B). FT-IR (cm⁻¹): ν_{BH} 2625 (m), 2582 (vs). MS (EI pos. 10 eV, *m/z*): 475 [M⁺] (100%). Anal. Calcd for C₁₈H₃₄B₁₀FeNOP: C, 45.48; H, 7.21; N, 2.95. Found: C, 45.31; H, 6.86; N, 2.78.

(S)-*N,N*-Dimethyl-1-[(R)-2-[(R)-1-(1,2-dicarba-closo-dodecaboran(12)yl)ethoxyphosphanyl]ferrocenyl]ethylamine ((S_C,R_P,R_{FC})-10). The same synthetic procedure as for the preparation and isolation of (R_P,R_{FC}/S_P,S_{FC})-8 was applied starting with (S_C,S_P,R_{FC})-4 (0.5 g, 1.07 mmol). Yield: 0.50 g (98%). Mp: 140–141 °C. ¹H NMR: δ 0.90 (d, ³J_{HH} = 6.8 Hz, 3H, CH(CH₃)N), 1.00 (t, ³J_{HH} = 7.0 Hz, 3H, OCH₂CH₃), 1.84 (s, 6H, NMe₂), 1.74–3.79 (m, v br,

Table 5. Crystal Data and Structure Refinement for Compounds 3–6

	(R _P ,S _{FC} /S _P ,R _{FC})-3	(S _C ,S _P ,R _{FC})-4	(R _P ,R _P ,S _{FC} ,S _{FC} /S _P ,S _P ,R _{FC} ,R _{FC})-5	(R _P ,R _{FC} /S _P ,S _{FC})-6
formula	C ₁₅ H ₂₇ B ₁₀ ClFeNP	C ₁₆ H ₂₉ B ₁₀ ClFeNP	C ₂₈ H ₄₂ B ₁₀ Cl ₂ Fe ₂ N ₂ P ₂	C ₁₅ H ₂₈ B ₁₀ FeNP
fw (g/mol)	451.75	465.77	759.28	417.3
<i>T</i> (K)	213(2)	213(2)	213(2)	213(2)
cryst syst	triclinic	orthorhombic	triclinic	monoclinic
space group	<i>P</i> 1	<i>P</i> 2 ₁ 2 ₁ 2 ₁	<i>P</i> 1	<i>P</i> 2 ₁ / <i>c</i>
<i>a</i> (Å)	7.2701(7)	7.3494(3)	10.2000(8)	7.1778(8)
<i>b</i> (Å)	18.926(2)	17.3675(7)	11.8589(9)	15.914(2)
<i>c</i> (Å)	19.101(2)	18.5680(8)	15.591(1)	19.423(2)
α (deg)	60.573(2)	90	73.318(2)	90
β (deg)	85.034(2)	90	84.707(1)	90.792(2)
γ (deg)	88.127(2)	90	80.770(1)	90
<i>V</i> (Å ³)	2280.4(4)	2370.0(2)	1781.0(2)	2218.4(4)
<i>Z</i>	4	4	2	4
<i>D_c</i> (g/cm ³)	1.316	1.305	1.416	1.249
μ (mm ⁻¹)	0.851	0.821	1.079	0.753
<i>F</i> (000)	928	960	780	864
cryst size (mm ³)	0.4 × 0.2 × 0.1	0.4 × 0.3 × 0.3	0.4 × 0.4 × 0.3	0.2 × 0.1 × 0.06
θ range for data collection (deg)	2.13–28.36	1.61–28.29	2.03–28.32	2.10–26.42
ranges of <i>h,k,l</i>	-9 ≤ <i>h</i> ≤ 9 -24 ≤ <i>k</i> ≤ 25 -25 ≤ <i>l</i> ≤ 25	-9 ≤ <i>h</i> ≤ 9 -22 ≤ <i>k</i> ≤ 23 -24 ≤ <i>l</i> ≤ 24	-13 ≤ <i>h</i> ≤ 13 -15 ≤ <i>k</i> ≤ 15 -20 ≤ <i>l</i> ≤ 19	-8 ≤ <i>h</i> ≤ 8 -19 ≤ <i>k</i> ≤ 19 -24 ≤ <i>l</i> ≤ 24
no. of reflns collected	21 228	21 603	19 114	15 939
no. of indep reflns (<i>R</i> _{int})	10 798 (0.0237)	5778 (0.0247)	8325 (0.0170)	4465 (0.0665)
no. of data/restraints/params	10 798/0/699	5778/0/367	8325/0/572	4465/0/365
GOF (<i>F</i> ²)	1.117	1.250	1.043	0.973
final <i>R</i> ₁ [<i>I</i> > 2 σ (<i>I</i>)]	0.0559	0.0404	0.0295	0.0475
<i>wR</i> ₂ (all data)	0.1223	0.0903	0.0852	0.1106
Flack param <i>x</i>		-0.004(16)		

Table 6. Crystal Data and Structure Refinement for Compounds 7–11

	($R_P, R_{FC}/S_P, S_{FC}$)-7	($R_P, R_{FC}/S_P, S_{FC}$)-8	($R_P, R_{FC}/S_P, S_{FC}$)-9	(S_C, R_P, R_{FC})-10	(S_C, R_P, R_{FC})-11
formula	C ₁₆ H ₃₀ B ₁₀ FeNOP	C ₁₇ H ₃₂ B ₁₀ FeNOP	C ₁₈ H ₃₄ B ₁₀ FeNOP	C ₁₈ H ₃₄ B ₁₀ FeNOP	C ₂₆ H ₄₈ B ₁₀ FeNOP
fw (g/mol)	447.33	461.36	475.38	475.38	585.57
T (K)	150(2)	180(2)	223(2)	213(2)	150(2)
cryst syst	monoclinic	monoclinic	monoclinic	orthorhombic	orthorhombic
space group	<i>P</i> 2 ₁ / <i>c</i>	<i>P</i> 2 ₁ / <i>c</i>	<i>C</i> 2/ <i>c</i>	<i>P</i> 2 ₁ 2 ₁ 2 ₁	<i>P</i> 2 ₁ 2 ₁ 2 ₁
<i>a</i> (Å)	10.087(2)	10.1289(6)	32.480(4)	11.2358(8)	9.3462(6)
<i>b</i> (Å)	8.615(2)	13.2285(8)	10.311(1)	13.1442(9)	17.693(4)
<i>c</i> (Å)	26.168(3)	36.317(2)	15.944(2)	17.377(1)	19.763(2)
α (deg)	90	90	90	90	90
β (deg)	91.83(1)	91.085(5)	104.883(3)	90	90
γ (deg)	90	90	90	90	90
<i>V</i> (Å ³)	2273.0(7)	4865.2(5)	5160.4(10)	2566.3(3)	3268.1(8)
<i>Z</i>	4	8	8	4	4
<i>D_c</i> (g/cm ³)	1.307	1.260	1.224	1.230	1.190
μ (mm ⁻¹)	0.743	0.696	0.658	0.662	0.532
<i>F</i> (000)	928	1920	1984	992	1240
cryst size (mm ³)	0.2 × 0.2 × 0.2	0.4 × 0.3 × 0.2	0.3 × 0.3 × 0.2	0.4 × 0.4 × 0.4	0.5 × 0.4 × 0.3
θ range for data collection (deg)	2.59–30.51	2.60–30.51	2.08–28.35	1.94–28.36	2.67–30.51
ranges of <i>h, k, l</i>	−14 ≤ <i>h</i> ≤ 14 −12 ≤ <i>k</i> ≤ 12 −37 ≤ <i>l</i> ≤ 37	−14 ≤ <i>h</i> ≤ 14 −18 ≤ <i>k</i> ≤ 18 −51 ≤ <i>l</i> ≤ 51	−43 ≤ <i>h</i> ≤ 42 −13 ≤ <i>k</i> ≤ 10 −21 ≤ <i>l</i> ≤ 21	−14 ≤ <i>h</i> ≤ 14 −14 ≤ <i>k</i> ≤ 17 −22 ≤ <i>l</i> ≤ 23	−13 ≤ <i>h</i> ≤ 13 −24 ≤ <i>k</i> ≤ 25 −28 ≤ <i>l</i> ≤ 28
no. of reflns collected	34 300	141 313	18 248	18 705	91 444
no. of indep reflns (<i>R_{int}</i>)	6912 (0.0354)	14831 (0.0494)	6037 (0.0277)	6170 (0.0241)	9966 (0.0281)
no. of data/restraints/params	6912/0/380	14 831/0/633	6037/0/425	6170/2/400	9966/0/553
GOF (<i>F</i> ²)	1.051	1.248	1.048	1.019	1.087
final <i>R</i> ₁ [<i>I</i> > 2(<i>I</i>)]	0.0320	0.0693	0.0378	0.0297	0.0243
<i>wR</i> ₂ (all data)	0.0790	0.1335	0.0814	0.0738	0.0618
Flack param <i>x</i>				−0.001(10)	−0.016(7)

10H, B₁₀H₁₀), 3.60 (m, 1H, OCH₂), 3.73 (m, 1H, OCH₂), 3.91 (q, ³*J*_{HH} = 6.8 Hz, 1H, CHMe), 3.91 (s, 5H, Cp), 3.96 (s, 1H, C₅H₃ *o* to CHN), 3.99 (m, 1H, C₅H₃ *m* to P and *m* to CHN), 4.08 (m, 1H, C₅H₃ *o* to P), 5.85 (s, br, 1H, C_{cluster}H). ¹³C{¹H} NMR: δ 7.1 (CHCH₃), 16.9 (d, ³*J*_{PC} = 9.2 Hz, OCH₂CH₃), 38.7 (NMe₂), 55.7 (CHN), 61.0 (C_{cluster}H), 68.8 (d, ²*J*_{PC} = 26.8 Hz, POCH₂), 70.1 (Cp), 71.0 (d, ³*J*_{PC} = 12.4 Hz, C₅H₃ *m* to P and *m* to CHN), 71.2 (C₅H₃ *o* to CHN), 74.5 (d, ¹*J*_{PC} = 15.0 Hz, C_{FC}P), 75.6 (d, ²*J*_{PC} = 50.7 Hz, C₅H₃ *o* to P), 78.1 (d, ¹*J*_{PC} = 97.6 Hz, C_{cluster}P), 92.2 (d, ²*J*_{PC} = 4.4 Hz, C_{FC}CHN). ³¹P{¹H} NMR: δ 143.0. ¹¹B{¹H} NMR: δ −11.1 (s, br, 6B), −9.1 (s, br, 1B), −8.4 (s, br, 1B), −1.2 (s, br, 1B), 0.1 (s, br, 1B). FT-IR (cm⁻¹): ν_{BH} 2640 (m), 2579 (vs). MS (EI pos. 14 eV, *m/z*): 475 [M⁺] (25.7%), 460 [(M − Me)⁺] (12.4%), 430 [(M − HNMe₂)⁺] (100%), 402 [(M − NMe₂ − Et)⁺] (10.8%), 332 [(M − C₂B₁₀H₁₁)⁺] (17.1%), 287 [(M − HNMe₂ − C₂B₁₀H₁₁)⁺] (24.2%), 212 [(FcCH=CH₂)⁺] (5.5%), 72 [(MeCH=NMe₂)⁺] (42.6%). Anal. Calcd for C₁₈H₃₄B₁₀FeNOP: C, 45.48; H, 7.21; N, 2.95. Found: C, 45.86; H, 7.21; N, 2.96.

(*S*)-*N,N*-Dimethyl-1-[(*R*)-2-[(*R*)-{1-(1,2-dicarba-closo-dodecaboran(12)yl)]-(1*R*,2*S*,5*R*)-2-isopropyl-5-methylcyclohexan-1-oxyl]-phosphanyl]ferrocenyl]ethylamine ((*S_C,R_P,R_{FC}*)-11). To (1*R*,2*S*,5*R*)-(−)-2-isopropyl-5-methylcyclohexanol ((−)-menthol) (0.5 g, 3.20 mmol), dissolved in *n*-hexane (30 mL), were successively added triethylamine (5 mL) and, in several small portions, solid (*S_C,S_P,R_{FC}*)-4 (0.5 g, 1.07 mmol). The mixture was stirred at room temperature overnight. Volatile substances including unconsumed (−)-menthol were removed in vacuo, and the residue was extracted three times with 20 mL portions of *n*-pentane. The extract was reduced in vacuo to a quarter of its volume and stored at −18 °C. Orange crystals, also suitable for X-ray analysis, grew over a few days. They were isolated by filtration, washed with a small amount of cold *n*-pentane, and dried. To increase the yield, the washing solution was combined with the mother liquor, concentrated again, and kept at −18 °C. Yield: 0.57 g (91%). Mp: 196–197 °C.

For assignment of ¹H and ¹³C NMR signals see Figure 8.

¹H NMR: δ 0.65 (m, 1H, H6a), 0.80 (m, 1H, H5a), 0.84 (d, ³*J*_{HH} = 5.5 Hz, 3H, H12), 0.90 (d, ³*J*_{HH} = 6.9 Hz, 3H, H10 or

H11), 0.95 (d, ³*J*_{HH} = 7.2 Hz, 3H, H10 or H11), 1.00 (d, ³*J*_{HH} = 6.8 Hz, 3H, H2), 1.14 (m, 2H, H5b and H8a), 1.28 (m, 1H, H8b), 1.46 (m, 2H, H7 and H6b), 1.74–3.79 (m, v br, 10H, B₁₀H₁₀), 1.94 (s, 6H, NMe₂), 2.55 (m, 1H, H9), 2.87 (m, 1H, H4), 3.93 (m, 1H, H3), 3.95 (s, 1H, C₅H₃), 3.99 (s, 6H, Cp and 1H of C₅H₃), 4.08 (q, ³*J*_{HH} = 6.8 Hz, 1H, H1), 4.14 (m, 1H, C₅H₃ *o* to P), 5.97 (s, br, 1H, C_{cluster}H). ¹³C{¹H} NMR: δ 8.2 (C2), 16.1 (C10 or C11), 21.4 (C10 or C11), 22.4 (C12), 22.9 (C7), 25.3 (C5), 31.9 (d, ⁴*J*_{PC} = 2.9 Hz, C9), 34.2 (C6), 39.0 (NMe₂), 43.0 (d, ³*J*_{PC} = 20.2 Hz, C4), 51.0 (d, ³*J*_{PC} = 3.9 Hz, C8), 55.4 (C1), 62.1 (C_{cluster}H), 70.3 (Cp), 70.8 (d, ³*J*_{PC} = 13.5 Hz, C₅H₃ *m* to P and *m* to C1), 71.3 (C₅H₃ *o* to C1), 74.9 (d, ¹*J*_{PC} = 20.0 Hz, C_{FC}P), 76.3 (d, ²*J*_{PC} = 56.0 Hz, C₅H₃ *o* to P), 78.7 (d, ¹*J*_{PC} = 103.7 Hz, C_{cluster}P), 80.1 (d, ²*J*_{PC} = 12.2 Hz, C3), 92.0 (d, ²*J*_{PC} = 4.6 Hz, C_{FC}C1). ³¹P{¹H} NMR: δ 128.2. ¹¹B{¹H} NMR: δ −11.1 (s, br, 6B), −9.0 (s, br, 1B), −7.8 (s, br, 1B), −1.0 (s, br, 1B), −0.3 (s, br, 1B). FT-IR (cm⁻¹): ν_{BH} 2669 (w), 2633 (m), 2586 (s), 2562 (s). MS (EI pos. 14 eV, *m/z*): 585 [M⁺] (62.1%), 540 [(M − HNMe₂)⁺] (100%), 403 [(M − NMe₂ − C₁₀H₁₈)⁺] (84.2%). Anal. Calcd for C₂₆H₄₈B₁₀FeNOP: C, 53.33; H, 8.26; N, 2.39. Found: C, 53.07; H, 8.08; N, 2.29.

X-ray Structure Determinations. Suitable crystals were mounted in perfluoropolyalkyl ether and cooled in a nitrogen stream. Crystallographic measurements were made using a Siemens SMART CCD diffractometer for compounds (*R_P,S_{FC}/S_P,R_{FC}*)-3, (*S_C,S_P,R_{FC}*)-4, (*R_P,R_P,S_{FC},S_{FC}/S_P,S_P,R_{FC},R_{FC}*)-5, (*R_P,R_{FC}/S_P,S_{FC}*)-6, (*R_P,R_{FC}/S_P,S_{FC}*)-9, and (*S_C,R_P,R_{FC}*)-10 and an Oxford Diffraction Xcalibur S diffractometer for compounds (*R_P,R_{FC}/S_P,S_{FC}*)-7, (*R_P,R_{FC}/S_P,S_{FC}*)-8, and (*S_C,R_P,R_{FC}*)-11. Data were collected using monochromatic Mo Kα radiation (λ = 0.71073 Å). The structures were solved by direct methods and refined on *F*² by full-matrix least-squares techniques (SHELX97).²³ All non-hydrogen atoms were refined anisotropically; hydrogen atoms were either located and refined isotropically or

(23) Sheldrick, G. M. *SHELX97* (includes *SHELXS97*, *SHELXL97*, *SHELXH97*), Programs for Crystal Structure Analysis (Release 97-2); University of Göttingen: Germany, 1997.

included in a riding mode. Figures show ORTEP depictions.²⁴ Crystal data and details of data collection and refinement are given in Tables 5 and 6. Further details are included in the Supporting Information.

(24) Johnson, C. R. *ORTEP*; Oak Ridge National Laboratory: Oak Ridge, TN, 1976.

Supporting Information Available: Crystallographic data for $(R_P, S_{FC}/S_P, R_{FC})$ -**3**, (S_C, S_P, R_{FC}) -**4**, $(R_P, R_P', S_{FC}, S_{FC}'/S_P, S_P', R_{FC}, R_{FC}')$ -**5**, $(R_P, R_{FC}/S_P, S_{FC})$ -**6**, $(R_P, R_{FC}/S_P, S_{FC})$ -**7**, $(R_P, R_{FC}/S_P, S_{FC})$ -**8**, $(R_P, R_{FC}/S_P, S_{FC})$ -**9**, (S_C, R_P, R_{FC}) -**10**, and (S_C, R_P, R_{FC}) -**11** as CIF files. This material is available free of charge via the Internet at <http://pubs.acs.org>.

OM700503T